YASAR UNIVERSITY
GRADUATE SCHOOL OF NATURAL AND APPLIED SCIENCE

POWER CONTROL IN A MICROGRID

Salisu Abdullahi

Thesis Advisor: Prof. Dr. M. Erol Sezer

Department of Electrical and Electronics Engineering

Presentation Date: 17/06/2015

Bornova-Izmir
2015

APPROVAL PAGE

This study entitle" POWER COTROL IN A MICROGRID"; a master thesis presented by Salisu Abdullahi, has been assessed in accordance with the relevance provision and requirement of Y.U Graduate Education and Training Regulations. The jury members have decided for this thesis defense and has been declared by majority of votes that the candidate has succeeded in his thesis defense examination dated 06/17/2015.

JURY MEMBERS	Signature
Prof. Dr. M. Erol Sezer	.....
Dr. Hacer Sekerci	...……..
Dr. Nurdan Yıldırım Özca	……..

ABSTRACT

POWER CONTROL IN A MICROGRID

Salisu Abdullahi

MSc. in Electrical Electronics Engineering

Supervisor: Prof. Dr. M. Erol Sezer

A micro-grid is a unifying of micro-sources together with a load and an optional energy storage device within a vicinity. The micro-grid can be operated in either autonomous, non-autonomous or a dual operation. In an autonomous operation micro-grid should generate its own energy and control it, as well. The components of the micro-grid which include 270kW of wind turbine, 40kW of micro-turbine, battery energy storage system with a capacity of 100kW and their control system have worked with each other in order to achieve power control in a micro-grid. The block diagram of the components and their parameters are made in a SIMULINK environment. The simulation test has been carried out by increasing the wind speed and decreasing the power demand in the system. Moreover, quick response of the battery energy storage system was observed in SIMULINK environment.

Keywords: Micro-grid; autonomous operation; micro-sources; control of power; modelling and simulation

Özet

BİR MICROGRIDDE GÜÇ KONTROLÜ

Salisu Abdullahi

Elektrik, Elektronik Mühendisliği

Gözetmen: Prof. Dr. M. Erol Sezer

Mikro şebeke, mikro kaynakların bir çevrede bir yük ve opsiyonel enerji depolama cihazıyla birleştirilmesine denir. Mikro şebeke ya otonom işlem, ya otonom olmayan işlem, ya da ikili işlemde çalıştırılabilir. Otonom işlemde mikro şebeke kendi enerjisini üretmeli ve aynı zamanda bu enerjiyi kontrol etmelidir. Mikro şebekenin bileşenleri olan 270 kW rüzgar türbini, 40 kW mikro türbin, 100 kW'lık pil enerji depolama sistemi ve bunların kontrol sistemi mikro şebekede güç kontrolü sağlamak için birbirleriyle çalışır. Bu bileşenlerin ve onların değişkenlerinin blok diyagramı Simulink ortamında oluşturulmuştur. Simülasyon testi sistemdeki güç talebinin azaltılıp rüzgar hızının artırılmasıyla gerçekleştirilmiştir. Bununla birlikte, Simulink ortamında pil enerji depolama sisteminin gecikmesiz tepkisi gözlemlenmiştir.

Anahtar Kelimeler; mikro şebeke, otonom işlem, mikro kaynaklar, güç kontrolü, biçimlendirme ve simülasyon

ACKNOWLEDGEMENT

I would like to thank Almighty Allah for his guidance and protection bestowed upon me throughout this period of my research.

A warmth gratitude and deepest appreciation to my advisor; Prof. Dr. M. Erol Sezer for his excellent guidance, understanding, patience, kindness and always supplying me with a good atmosphere for conducting this research. He shows me how to carry out a good research independently.

I would also like to extend my gratitude to all the faculty staffs of Electrical Electronics Engineering department, more especially those that have taught me different fields of knowledge horizon in various capacities.

A special thank goes to my parents, brothers and sisters. Their prayers, love, support and words of encouragement that sustain me thus far. I will forever remain grateful.

Finally, I would like to acknowledge the support and advice I received from friends. I appreciate all your efforts and understanding.

Thank you all

TABLE OF CONTENTS

Page

INDEX OF FIGURE

FIGURE Page

INDEX OF TABLE

TABLE Page

SYMBOL AND ABBREVIATION

Abbreviation	Explanation
MC	Micro sources controller
CC	Central controller
CHP	Combine heat and power
P.U	Per unit
CB	Circuit breaker
LV	Low voltage
μ	Micro
μT	Micro turbine
PV	Photo voltaic
PLL	Phase-lock loop
FC	Fuel cell
WT	Wind turbine
PCC	Point of common couple
CO_2	Carbon dioxide
SOC	State of the charge
SGCC.	State Grid Corporation of China

μG	Micro grid
IREC	International Institute for Energy Research
IREL	National Renewable Energy Laboratory
NASA	National Aeronautics Space Administration
AC	Alternative current
DC	Direct current
BESS	Battery Energy Storage System
RPM	Revolution per minutes
PI	Proportional Integral
PID	Proportional Integral Derivative
PWM	Pulse Width Modulation
IG	Induction Generator
AGC	Automatic Gain Control
PEV	Plug-in electric vehicle
MTN	Micro-turbine node
WTN	Wind-turbine node
LDN	Load node
SC	Synchronous Condenser

Symbol

A	Turbine sweep area (m^2)
B_{rated}	Battery rated (Ah)
C	Capacitance (F)
C_1	Capacitance of the buck mode (F)
C_2	Capacitance of the boost mode (F)
C_P	Performance coefficient (-)
C_f	Filter capacitance (F)
D_{boost}	Modulation index of boost mode (-)
D_g	Damping of the generator (-)
D_t	Damping of the turbine (-)
f	Nominal frequency (Hz)
F_g	Generator friction (-)
F_s	Switching Frequency (Hz)
$F_{wt,sc}$	Frictional factors of both WT and SC (W)
G_S	Wind generator speed (m/s)
H	Moment of inertia (-)
I_{abc}	Line currents (A)

I_b	Battery current (A)
$I_{discharge}$	Discharge current (A)
I_{dc}	Current at dc-link level (A)
I_o	Load current (A)
J	Generator inertial ($kg.m^2$)
K	Modelation index (-)
k	Unity factor (-)
K_i	Integral gain PI controller (-)
K_L	Coefficient estimated of ripple current (-)
K_P	Proportional gain PI controller (-)
K_T	Tempreture control loop (-)
L	Inductance (H)
L_f	Filter inductance (H)
L_{max}	Load limit (-)
Lm	Mutual inductance (H)
Lr	Inductance of rotor circuit (H)
Ls	Inductance of stationary circuit (H)
P_d	Power loss due to damping (W)

P_e	Electrical power output (W)
P_g	Gas power (W)
P_m	Mechanical power (W)
P_n	Number of pole (-)
Pn,wt,sc	Number of poles of WT and SC (-)
P_{rated}	Power rated (W)
P_{ref}	Power reference (-)
P_{sc}	Apparent power of SC (W)
P_{wt}	Apparent power of WT (W)
P_w	Wind power (w)
Q	Operating charge (Ah)
Q_c	Critical charge (Ah)
Q_e	Exponential Capacity (Ah)
Q_m	Maximum capacity (Ah)
Q_n	Nominal capacity (Ah)
Q_o	Fully charge (Ah)
R_b	Battery internal resistance (Ω)
R_r	Resistance of a rotor part (Ω)

R_s	Resistance of a stationary part (Ω)
T_1	Fuel system lag time constant 1(s)
T_2	Fuel system lag time constant 2 (s)
T_3	Load limit time constant 3 (s)
v	Wind speed (m/s)
V_{abc}	Line voltages (V)
V_b	Battery open circuit voltage (V)
V_{br}	Ripple voltage desire at buck mode (V)
V_{dc}	DC-voltage (V)
V_{dcr}	Ripple voltage desire at book mode (V)
V_e	Exponential Voltage (V)
V_f	Full-charge voltage (V)
V_n	Nominal Voltage (V)
V_{max}	Maximum value position (-)
V_{min}	Minimum value position (-)
V_o	Load voltage (V)
$V_{o,av}$	Total harmonic load voltage (V)
V_{rated}	Voltage rated (V)

Greek letters

β	Blade pitch angle (deg)
ρ	Air density (kg/ m^3)
ω	Operating frequency (Hz)
ω_o	Rated frequency (Hz)
ω_m	Shaft speed (rad/s)
$\dot{\omega}_m$	Shaft speed rate (rad/s^2)
ω_r	Rotor speed (rad/s)
ρ	Air density (kg/ m^3)
γ	Tip speed ratio (-)

1 INTRODUCTION

1.1 Description of a Micro-Grid

A micro-grid (μG) can be defined as a small power generation and distribution system capable of supplying regulated power to a local load. The μG is normally erected on an island or a remote rural area where there is an absence of the main grid or because of a long distance to reach the distribution and transmission framework. These can help to reduce the transmission power losses from the main grid and provided a good power to the consumers. Also the μG has the capability to supply uninterrupted power, thus more reliable for critical areas like military bases and hospitals. The potential of the μG to integrate many micro-sources close to one another to generate electricity help to eliminate the emission of CO_2 along its cost.

1.2 General Structure of a Micro-Grid

A general μG architecture is shown in Fig. 1.1. The μG consist of three feeders namely; A, B and C. Combine heat and power (CHP) sources, non-CHP sources, loads, heat loads, two sensitive loads, one insensitive load and storage devices were connected on A and C, while and B caries only the loads. They have combined the two micro-sources and one storage device close to each other for minimizing the heat and power losses. Micro-sources are capable of supplying both power and heat to the loads. The micro-sources can be isolated or connected from the feeders by ON and OFF switches accordingly.

Also the feeders A and C may be disconnected or connected to the μG through circuit breakers (CB_1-CB_2). The other feeder B is supplied with power only to the non-sensitive loads through an on/off circuit breakers. If the main grid has a problem or it is disconnected from μG, the feeder B would not be able to supply power to it's local loads. The μG has been connected to the main grid through the point of common coupling (PCC) which acts as a circuit breaker (CB_4) [1]. If a

problem occurs in the main grid, the μG will be automatically disconnected from it through the PCC. The PCC may be used to connect or disconnect μG from the main grid. In a grid connected mode, power could be transferred or received from the μG through PCC. The CC has been controlling the entire energy sources and their local loads in the μG. In island mode, the μG should be able to generate it is own energy and control it.

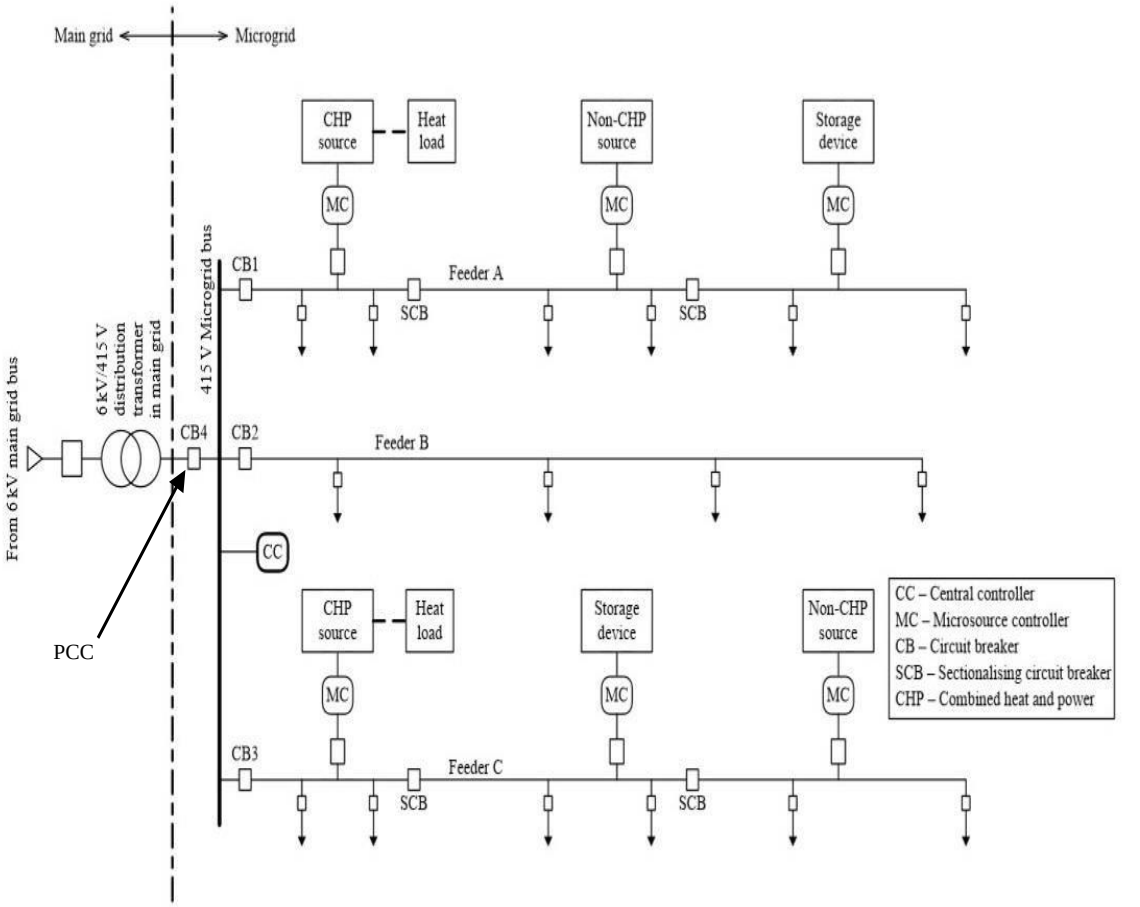

Fig 1.1. Typical Configuration of a μG [1].

1.3 Examples of µG

In this section, examples of µG's with their similarities and differences from different countries which include China, Greece, India, Spain and Japan are presented.

China

As shown in Fig. 1.2 below, the largest µgrid in Zhangbei-China with 160 MW which include a wind turbine of 100MW, a PV cell of 40MW, a main grid connected and a battery energy storage system of 20MW.

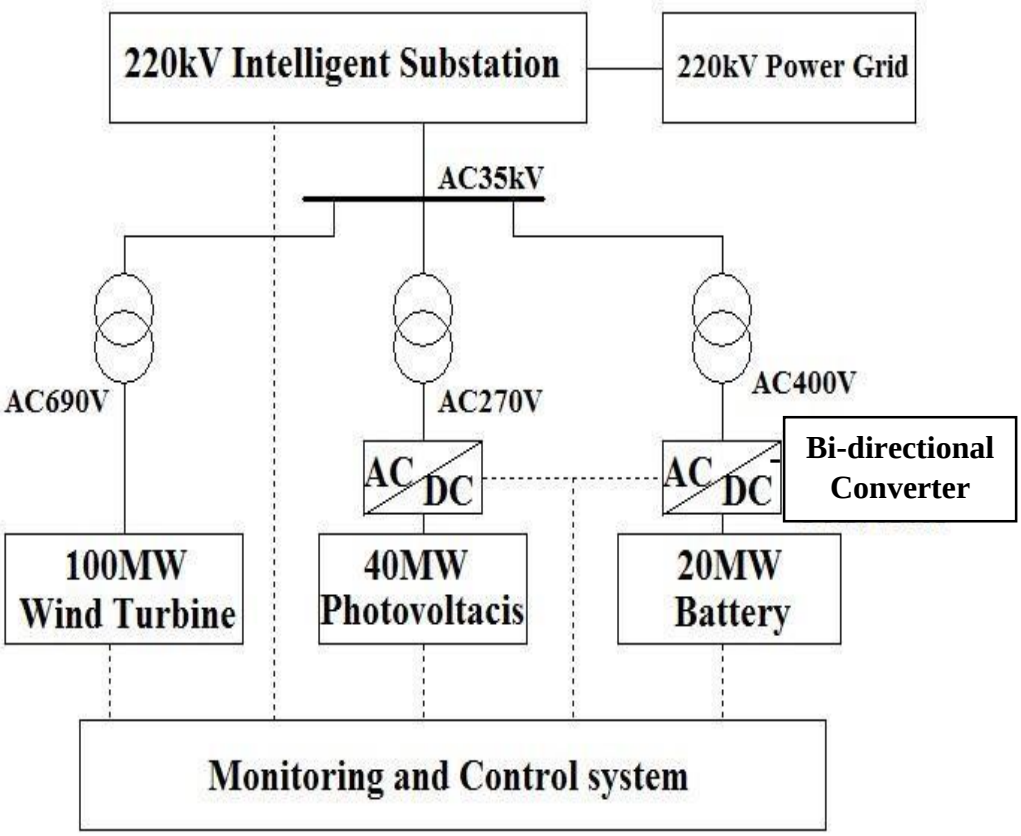

Fig.1.2. Micro-Grid in Zhangbei-china [2]

Greece

In Greece the Kythnos comprises a diesel generator, a PV cell and bank of a battery is located on an island of the Cyclades Archipelago of the Aegean Sea [3]. This μG can be used to supply the demand power of 12 houses on the island. The battery power could be balanced between loads and micro sources, if it is needed. The μG of Kythnos site is shown in Fig 1.3

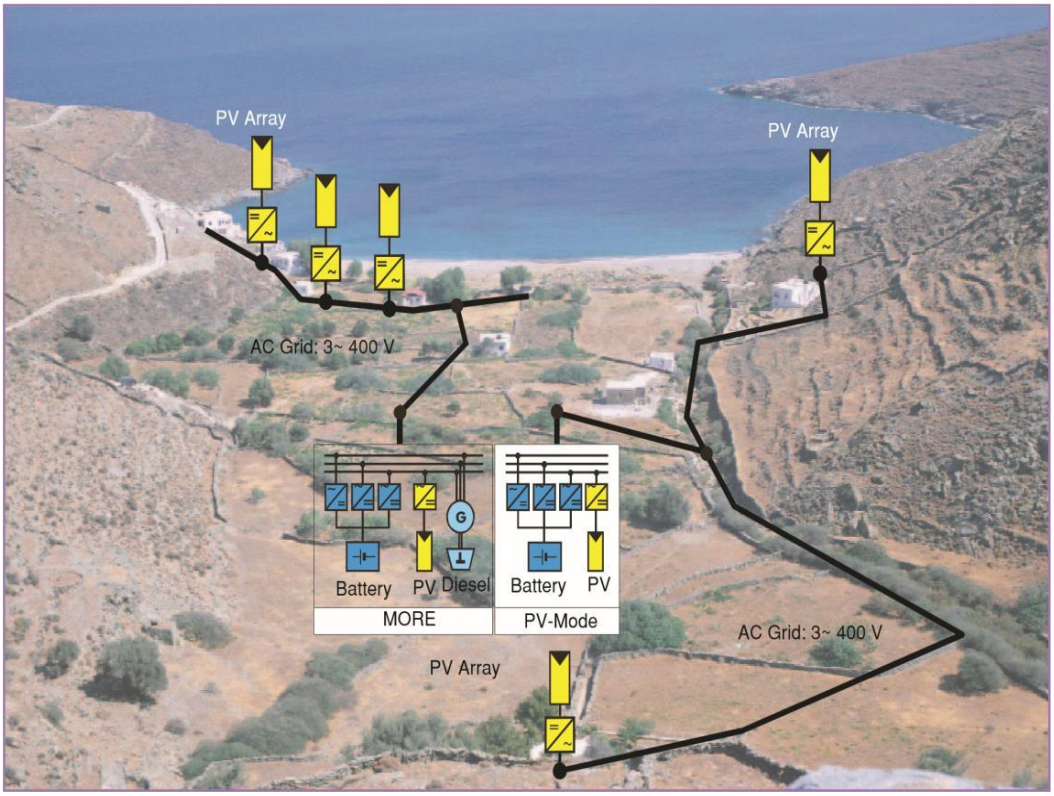

Fig 1.3. μG of Kythnos [3]

Spain

The μG of the Catalonia Institute for Energy research (IREC) is situated in Barcelona-Spain. It has a capacity of 200kW and its single line diagram is presented in Figure 1.4. The IREC's μG components are emulated system, the real system,

semi-emulated system and others with their rated values and description as cited in [4]. The first, the second and the third units on a single line diagram of IREC's μG are representing a wind power generation, a storage device and a consumer's node respectively. The only difference from this μG and others is that, the plug-in electric vehicle (PEV) could supply power to the IREC's μG or vice versa.

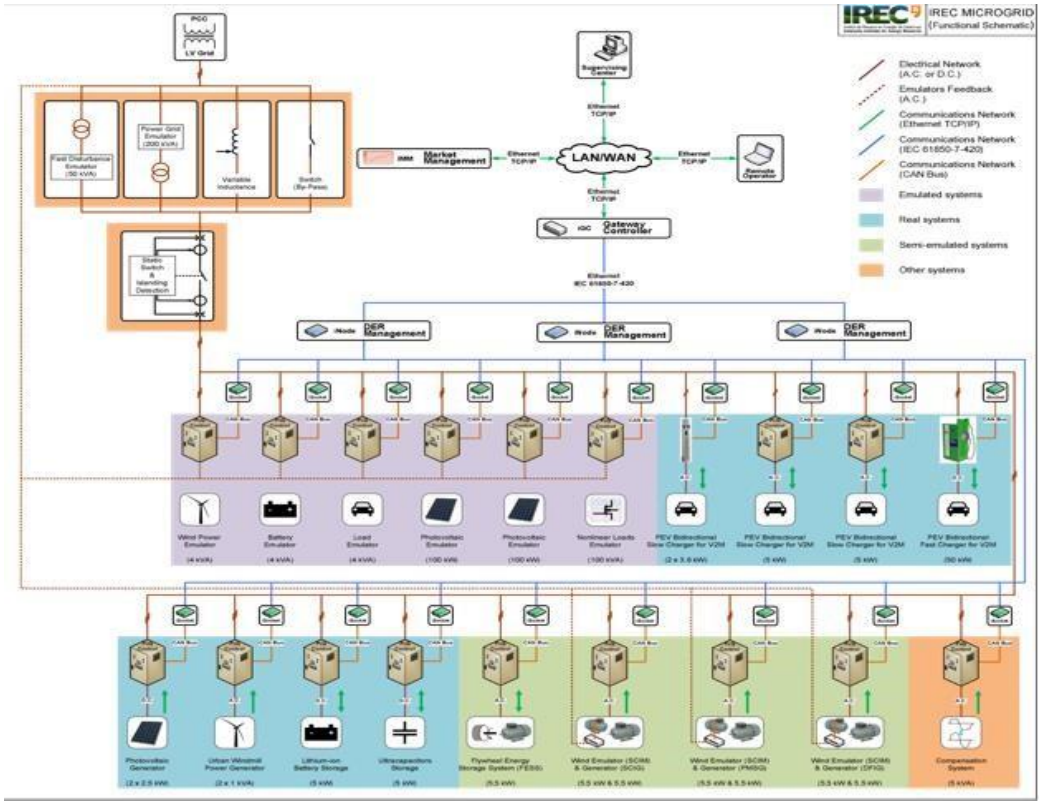

Fig 1.4. Single Line Diagram of IREC [4].

Japan

In [5], an islanded μG was formed with an existence of diesel generator, a PV cell, a wind turbine and a storage energy system of both lead acid and lithium batteries. The island μG is placed in six villages of Kyushu; Kuroshima, Takeshima, Nakanoshima, Suwanosejima, Kodakarajima and Takarajima located in Japan. Each of this island has an existence of PV and diesel generator. They have fluctuations problems in both PV and loads site because of the generator inertia problem. To solve these issues, a μG has to be considered. A wind turbine of 10kW and PV of 60kW integrated together

with an existence of power station of 240kW to form a µG for Kuroshima Island shown below.

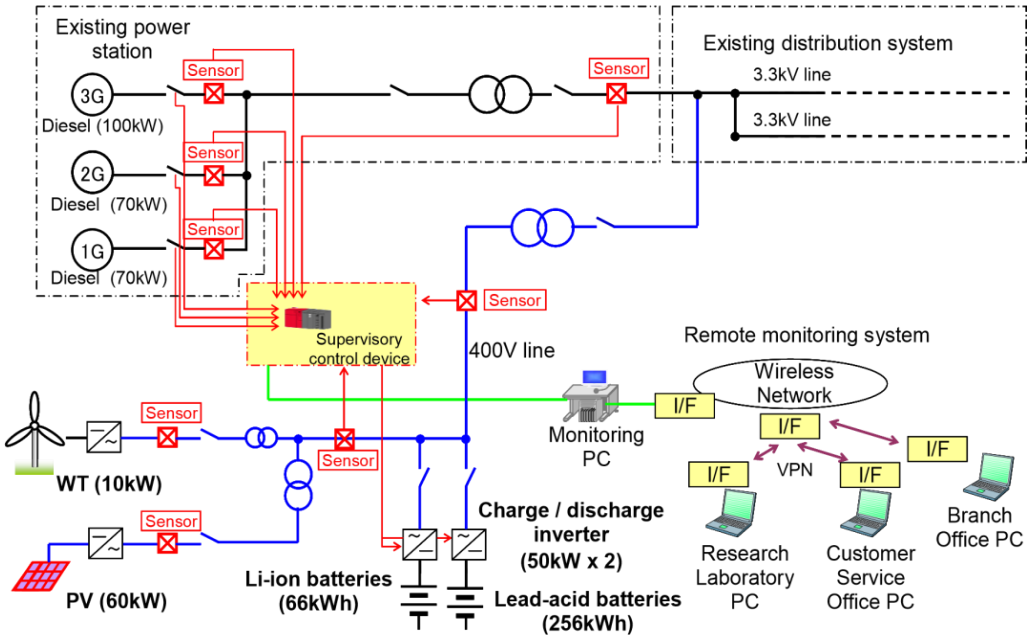

Fig 1.5. Installed µG of kuroshima island [5].

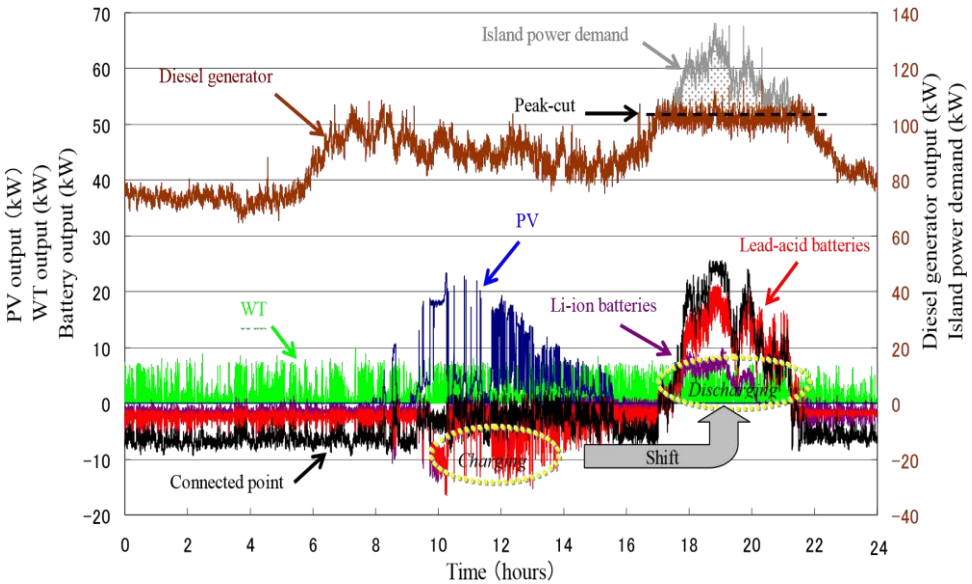

Fig 1.6. Power exchange among µsources [5]

Maldives-India's Ocean

In a remote area of the republic of Maldives-India's Ocean that consist of Uligam, Raimandhoo and Kondey islands have a three implemented µgrids system with 24×1.8kW wind turbine, 30kW of an existence diesel generator and PV cells for 2.5kW to each island. But here only Uligam Island has been considered. In those days, they were using only a diesel generator as a source of energy. They have decided to establish a µG in order to reduce the diesel price and provide a good power to their consumers. The high demand of a diesel generator is charged about 9L/h for each 30kW. As a result of that, they had proposed a µG with the above µsources together with an existence of the diesel generator as shown below.

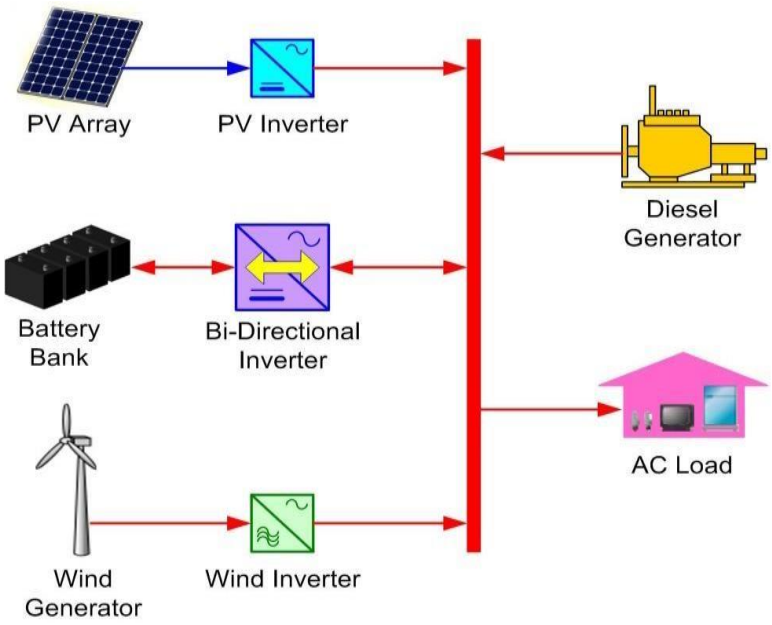

Fig 1.7. Single Line Diagram of Uligam Island [6].

The basic information on this island needs to be taken through a leader of the community. The information such as best wind location of 4.5^0 north latitude (NLat) to 6.5^0 NLat and cost per unit like 9L/h of the electricity from the consumer's side is calculated.

Similarities and Differences

The similarities of countries' μG are selected based on their components which are Bi-directional inverted, monitoring and control centre, photovoltaics cells, batteries and loads. Also the differences were picked according to diesel generator connection with main-grid and PEV.

Table 1.1. Comparison of the components

Countries	Components
China	battery, photovoltaic cell, load, main-grid and wind-turbine
Spain	battery and capacitance, photovoltaic cell, load, PEV and wind-turbine
Greece	battery, photovoltaic cell, load, and diesel generator
Maldives-India's Ocean	battery, photovoltaic cell, load, wind-turbine and diesel generator
Japan	battery, photovoltaic cell, load, and wind-turbine

The only similarities base of their components among the countries' μG are photovoltaics, batteries and loads and their differences according to the table above as clearly shown are PEV, wind-turbine and Diesel generator connected to the main grid.

1.4 Literature review

A control techniques for distribution generation together with CHP in a μG was presented in [7] by Robert H. Lasseter and Fellow, IEE Professor Emeritus. In [8], a Senior IEEE member Zhenhua Jiang described the control method of power sharing and voltage between parallel inverter-interfaced in an islanding operation by using drop control scheme. In [9], Rashad M Aymen Chaouachi and Ken Nagasaka studied different control strategies of transient dynamic response of two μG close to each other. If the large disturbance was occurring in the main grid, the automatic gain control change the operation mode automatically. In [10], Rashad M. Kamel, Aymen Chaouachi and Ken Nagasaka analyzed the stability of μG based on the import and export of active and reactive power from or to the main grid by control strategies of active and reactive power. In [11], Manohar Chamana and Stephen B. Bayne discussed another respond for changing the mode of operation between main grid and μG through master slave control method. The control, coordination of changes in DG, load and structure in a μG and power quality under different disturbance in the system was discussed by Li Bin, Bao Hailong and Chenyao in [12]. In reference [13], Gelu Gurguiatu1 Ionel Vechiu and toader Munteanu Presented a control function of active power conditional (APC) as an interface between renewable energy source and μG for improving power quality through phase-lock loop (PLL).

1.5 Organization of thesis

The structure and organization of this thesis has been stated as follows: In **chapter one**, the introduction of the μGrid together with μsources has been established. The example of an existing project from different countries along with their components also been discussed. Next to this is the literature review of relevant researches and findings presented. The coordination of this work is situated. The general structure of the μGrid and the details are presented in **chapter two**. The components of μGrid also are well defined. The details of elements used in this work is documented. In **chapter three**, the Simulink diagrams of μsources and storage device with their parameters was presented. The simulation results of different configurations based on μGrid diagram are shown. Finally, in **chapter four** the discussion and conclusion of the previous results in conjunction with the future work is clearly revealed.

2 DESCRIPTION OF THE SYSTEM STUDIED

The single-line diagram of the micro-grid studied in this work is shown in Fig. 2.1. It includes a wind turbine as the main power source, a micro-turbine and a battery as back-up sources, all feeding a local load. The battery is connected to the grid by a bi-directional inverter that facilitates transfer of power to and from the battery as needed. A synchronous condenser is added to the grid to provide reactive power to the both load and induction generator (IG) respectively.

In the following of this chapter detailed models of the components involved are given.

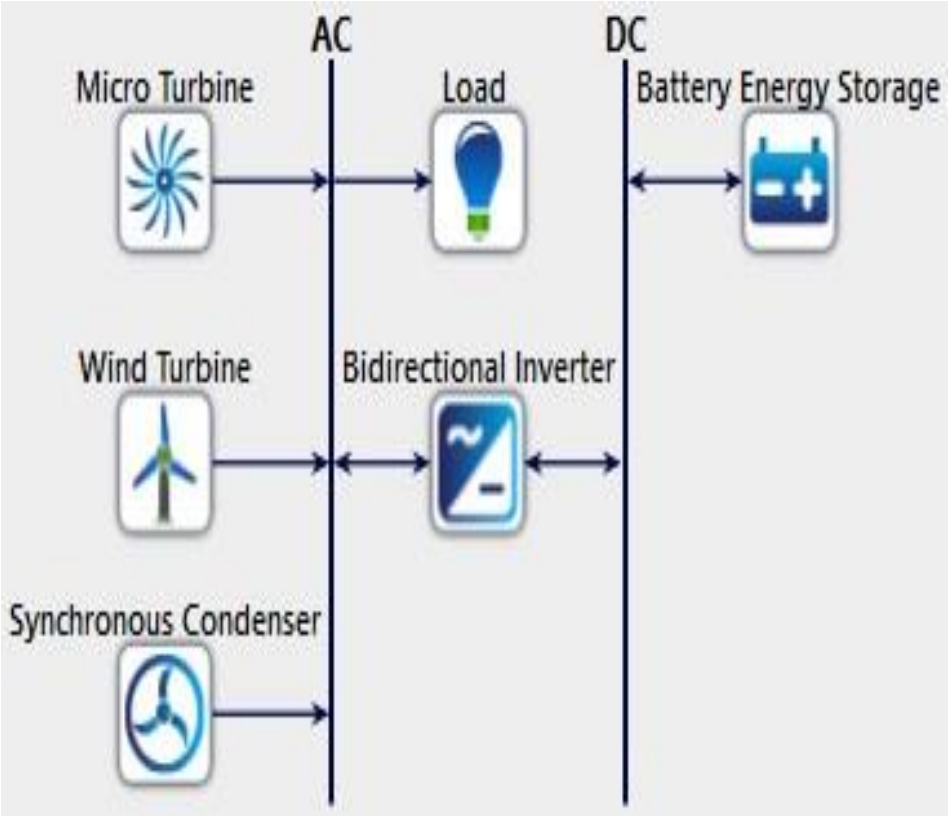

Fig 2.1. Single-Line Diagram of The μG Studied

2.1 Wind -turbine Model

The mechanical power produce by a wind turbine is given [14] by

$$P_m = C_p(\beta,\gamma)\frac{\rho A}{2} v^3 \quad (1)$$

The performance coefficient, depends on two parameters: blade pitch angle and tip speed ratio and is given as

$$C(\beta,\gamma) = 0.22\left(\frac{116}{\gamma i} - 0.4\beta - 5\right)e^{-\frac{12.5}{\gamma i}} \quad (2)$$

where

$$\frac{1}{\gamma i} = \frac{1}{\gamma + 0.08\beta} - \frac{0.035}{\beta^3 + 1} \quad (3)$$

In this study, we assume that there is no blade pitch control, and accordingly set $\beta = 0$. Then, for fixed ρ and A, Pm becomes a function of γ and v. Typical power characteristics of such a wind turbine for varying wind and turbine speeds are shown in Fig.2.2.

In this work, the wind turbine is assumed to be operated in a small range of a turbine speed determined by the frequency as shown in the figure below.

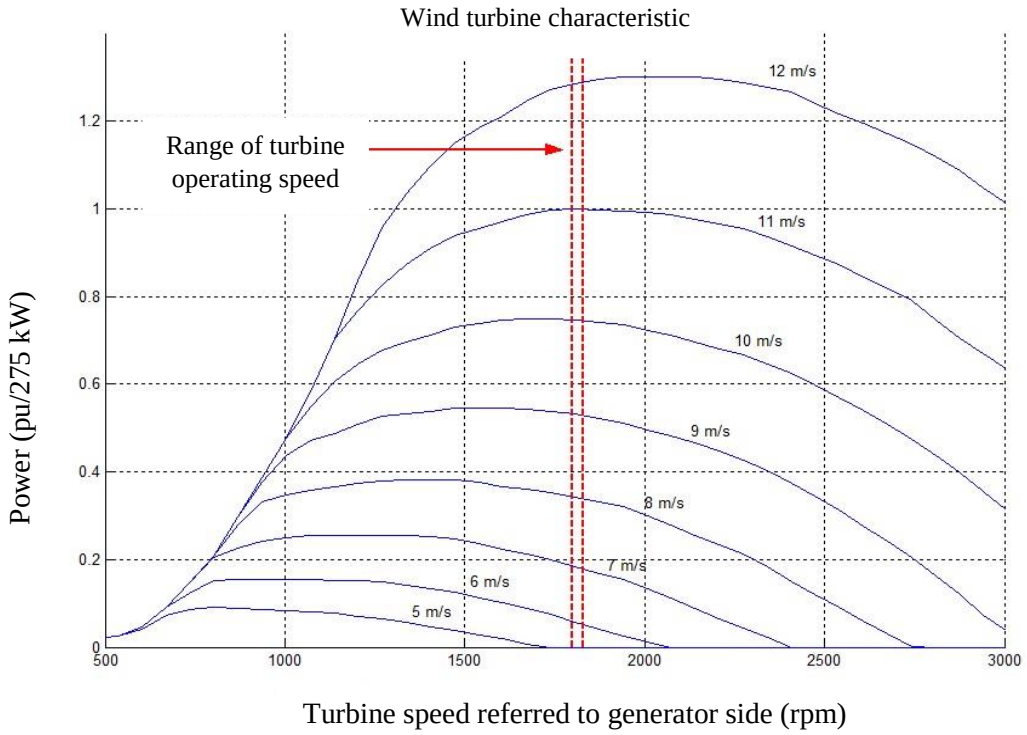

Fig 2.2. Typical Wind Turbine characteristic [15].

The wind turbine is connected to an IG through a gear-box as shown in Fig. 2.3, where P_W, P_m, P_t and P_e denote the wind power, mechanical output power of the turbine, mechanical input power to the generator, and the electrical output power of the generator. Assuming that the power loss in the gear-box is negligible, we take $P_t = P_m$.

The dynamics of the IG is governed by [16].

$$2H\,\omega_m \dot{\omega}_m = P_m - P_e - D_g \omega_m (\omega_m - \omega) \tag{4}$$

and all quantities are given in normalized (p.u) values.

Thus, the model of the wind turbine including the induction generator is obtained as shown in the block-diagram in Fig.2.3.

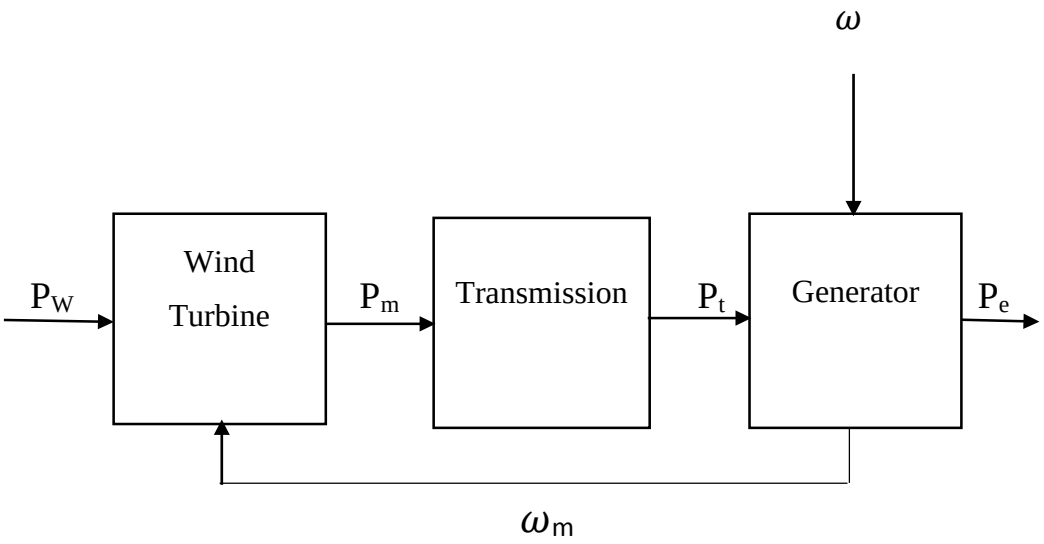

Fig 2.3. Wind turbine main block model

2.2 Micro-turbine Model

The micro-turbine has a considerably smaller power rating as compared with the wind turbine. It's role is to provide the excess power demand due to a small increase in the load or a small decrease in the power generated by the wind turbine as a result of reduced wind speed.

In this work, we consider a gas turbine that also produces heat used for other purposes. Such turbines are high-speed turbines that are connected to the generator either directly (single-shaft) or through a gear-box (split-shaft). The single-shaft turbine requires further power electronics to reduce the frequency of the generated electrical power (in the kHz range) to the grid frequency [17]. In the split-shaft turbine, generator shaft speed is suitable for direct connection to the μG [16].

In this work, split-shaft turbine is adopted. It is connected to μG through an IG just like the wind turbine. The overall block-diagram of the micro-turbine / generator system is similar to the wind-turbine / generator system shown in Fig. 2.3, except that the wind turbine is replaced with micro-turbine, and the wind power P_w is replaced with the gas power P_g input to the turbine.

The IG has the same dynamics as one that is connected to the wind-turbine with the different H and D parameters.

The micro-turbine is described by two first order lags, one associated with the combustor and the other with turbine. Roughly,

$$P_m = \frac{K}{(1 + \tau_1 s)(1+ \tau_2 s)} P_g - P_d \quad (5)$$

where

P_d : power loss due to damping and given as

$$P_d = D_t \omega_m \quad (6)$$

where D_t is the overall damping of the turbine.

Thus the block-diagram of the micro-turbine is obtained as shown in Fig.2.4.

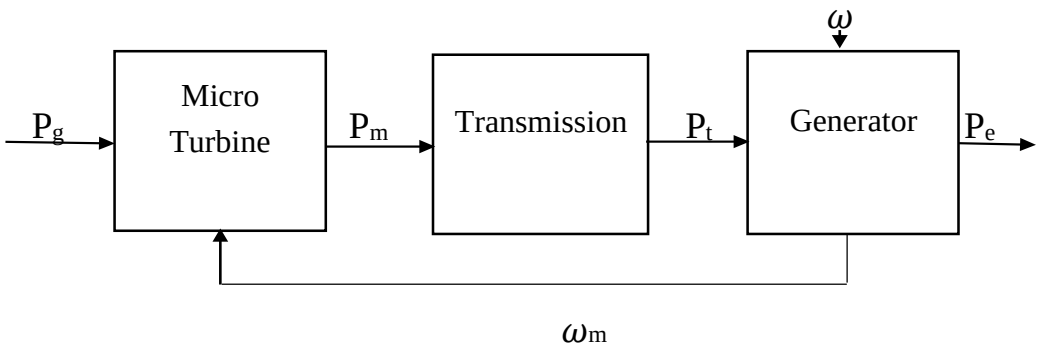

Fig.2.4. Block Diagram of Micro Turbine (Similar to fig 2.3)

The micro-turbine also includes a two-mode controller that adjusts the gas input power to satisfy the electrical power demand from the turbine. If the battery is connected to the μG (mode 1), then the frequency and the voltage of the μG is regulated by the controller circuitry of the battery as will be explained later. In this mode of operation, the role of the micro-turbine is to produce power to recharge the battery if the battery charge drops below a preset value until it is fully charged after which micro-turbine is shut down. If the battery is disconnected (mode 2) from the grid for any reason (malfunction, maintenance, etc.), then the controller is

responsible from the regulation of the frequency. The block-diagram of the controller is given in Fig.2.5, where

$Q/Q_O/Q_C$: Operating / full / critical charge of the battery.

ω/ω_o : operating / rated frequency of the μG.

LC_1 / LC_2 : Local controllers for mode 1/2 operation

PM_1 / PM_2 : Mechanical power demand for mode 1/2 operation

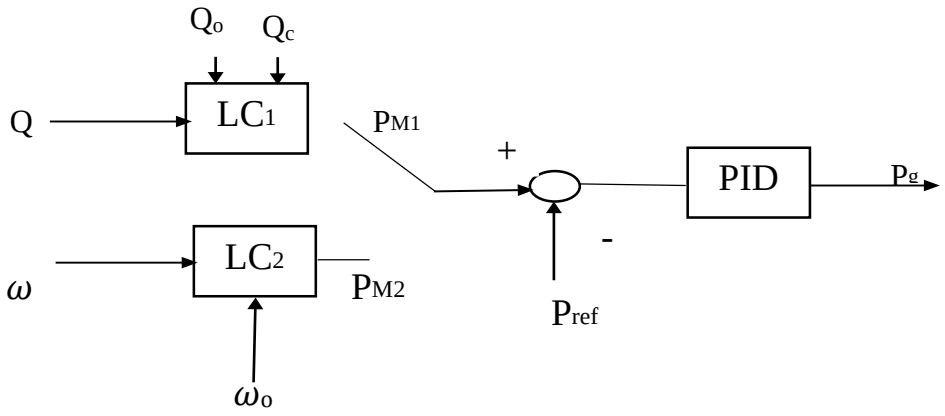

Fig.2.5. Controller of the Micro-Turbine

2.3 Battery model

The battery, which is the immediate back-up source, is connected to the μG through a boost-buck converter, a bi-directional inverter and LC filter as shown in Fig.2.6.

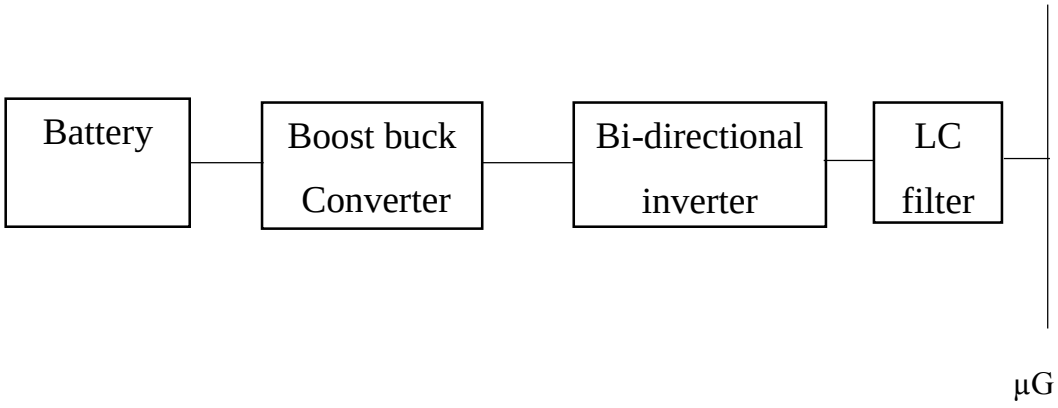

Fig.2.6. The Battery and Associated Units

The lead-acid battery has the nominal discharge characteristics shown in Fig.2.7.

It is assumed that the battery has the same charge and discharge characteristics, although they differ slightly in actual operation. The V-Q curve (discharge curve) also depends on the discharge current due to the internal resistance of the battery.

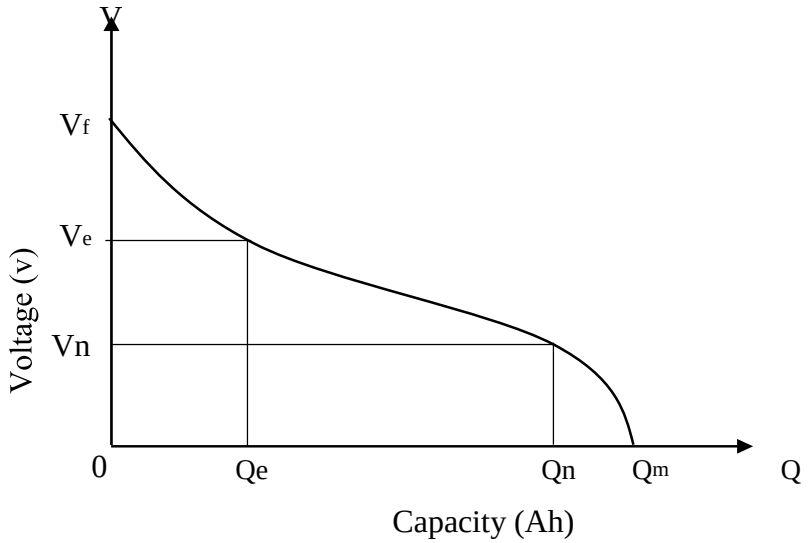

Fig.2.7. Discharge Curve

As the term used indicate, the voltage drops from V_f to V_e exponentially in the exponential zone, then from Ve to V_n almost linearly in the nominal zone, and finally from V_n to zero abrubtly with further discharge. Equation relating V to Q and discharge current I can be found in [18].

The boost-buck converter is used to regulate the DC link voltage, and has the structure shown in Fig.2.8. The MOSFETS Q_1 and Q_2 are driven by a pulse width modulation (PWM) signal with a controlled duty-cycle, and either one or the other is ON depending on V_{dc} is above or below a reference value. Thus V_{dc} is kept constant irrespective of the battery voltage and whether it is being charged or discharged.

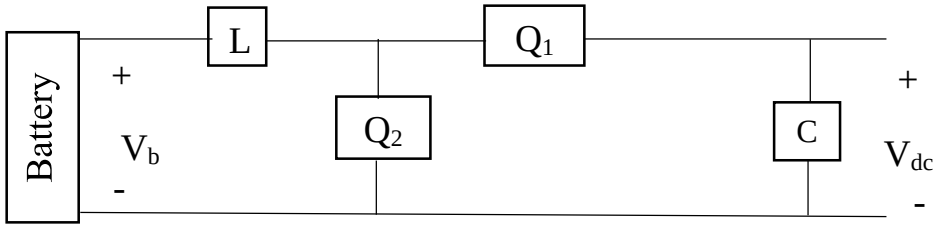

Fig.2.8. The Boost-Buck Converter

The magnitude of inductance and capacitor parameters of boost-buck converter can be calculated as follows [19].

$$L = \frac{(V_b \times (V_{dc} - V_b))}{(I_b \times f_s \times V_{dc})} \quad (7)$$

$$C_1 = \frac{(K_L \times I_b)}{8 \times f_s \times V_{br}} \quad (8)$$

$$C_2 = \frac{(D_{boost} \times I_{dc})}{(f_s \times V_{dcr})} \quad (9)$$

The three-phase bi-directional inverter facilitates power transfer between the DC link and AC μG. It consists of six MOSFETS switches, two per phase, which are controlled by a PWM voltage generated by the main v/f controller. A single-line diagram of such an inverter is shown in Fig.2.9.

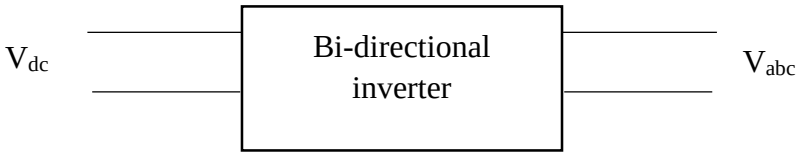

Fig.2.9. Bi-directional Inverter

The three-phase filter shown in Fig.2.10 eliminates the harmonic generated by the inverter.

Fig.2.10. LC Filter.

The value of the inductors and capacitor of the filter are calculated as [20].

$$K = \{\frac{k^2 - \frac{15}{4k^4} + \frac{64}{5\pi k^5} - \frac{5}{4k^6}}{144}\}^{1/2} \quad (10)$$

$$L_f = \frac{V_0}{I_0 \times F_s}\{K\frac{V_{dc}}{V_{0,av}}[1 + 4\pi^2(\frac{f}{Fs})^2 K\frac{V_{dc}}{V_{0,av}}]\}^{1/2} \quad (11)$$

$$C_f = \frac{V_{dc}}{L_f F^2{}_s V_{0,av}} \quad (12)$$

2.4 Asynchronous Condenser

Synchronous condenser is a synchronous machine with an exciter in which it is mechanically input is zero. The mechanical input is not connected to anything rather than spin freely. However, it works in order to supply enough reactive power to the whole system.

2.5 Main V/f Controller

The function of the main V/f controller is to regulate the voltage and frequency of the μG by controlling the PWM generator of the bi-directional inverter when the μG is operating in islanding mode. Frequency is calculated from three-phase voltage and current measurements using a PLL. The deviations of frequency and voltage are modified by proportional-integral-derivatives (PID) controllers to adjust the PWM. A simplified block diagram of the main V/f control unit is shown in Fig 2.11. Detailed SIMULINK diagram is given in chapter three.

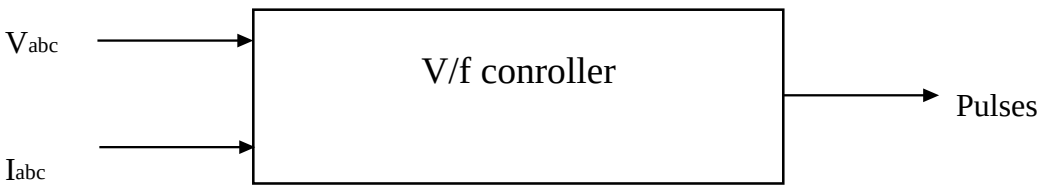

Fig.2.11. V/f Controller

3 DETAILED SIMULINK DIAGRAM

3.1 SIMULINK Model of the Micro-Grid

The overall SIMULINK model of the μG is shown in Fig.3.1, where WTN, MTN, BTN and LDN are connection nodes of the wind-turbine, micro-turbine, battery and the load to the μG. For simulation purposes two different loads are considered: when circuit-breaker BRK is open, load 1 is the only load, when BRK is closed, total load is the parallel connection of load 1 and load 2.

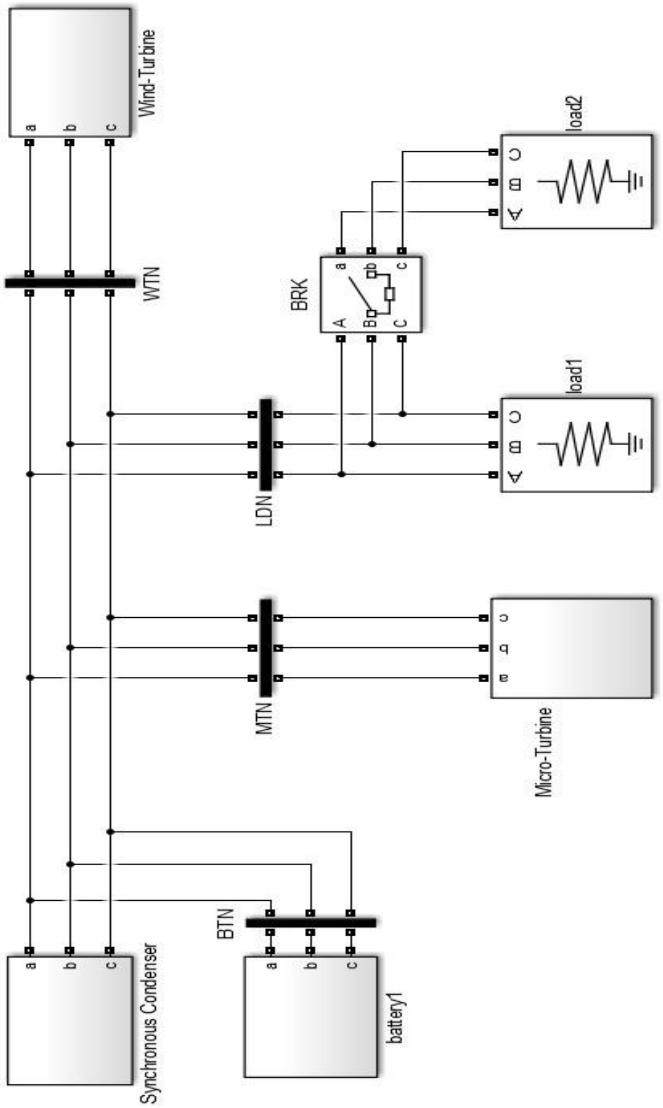

Fig.3.1. General Structure

The wind-turbine unit consists of a wind-turbine block and IG block as shown in Fig.3.2. The rotor speed of the IG is selected from the output vector (m) of the IG to be fed into the WT block, whose second input, the wind speed, is provided externally.

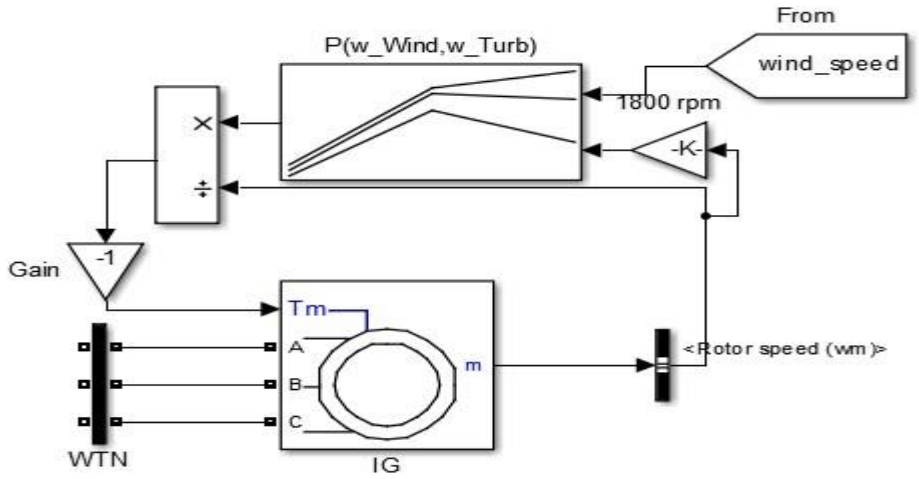

Fig.3.2. Wind-Turbine

The SIMULINK model of the micro-turbine unit is shwon in Fig.3.3. The micro-turbine is constructed from SIMULINK block as enclosed by the dashed rectangle in Fig.3.3, and a library block is used for the induction generator.

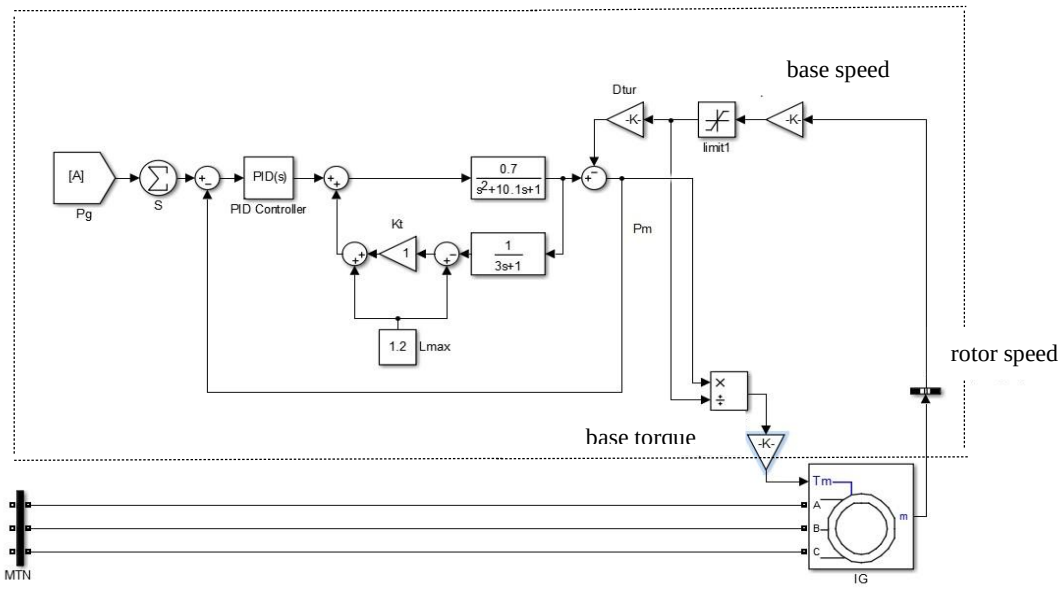

Fig3.3. Micro Turbine.

The battery unit consist of the battery, the boost-buck converter, the bi-directional inverter and the filter whose SIMULINK model are given in Figs.

3.4-3.7. Fig. 3.4 simply simulates the discharge characteristics. In Fig 2.7, and all models are constructed using library blocks.

In Fig.3.4, the battery voltage is created from SIMULINK blocks and it's explained in section 2.3.

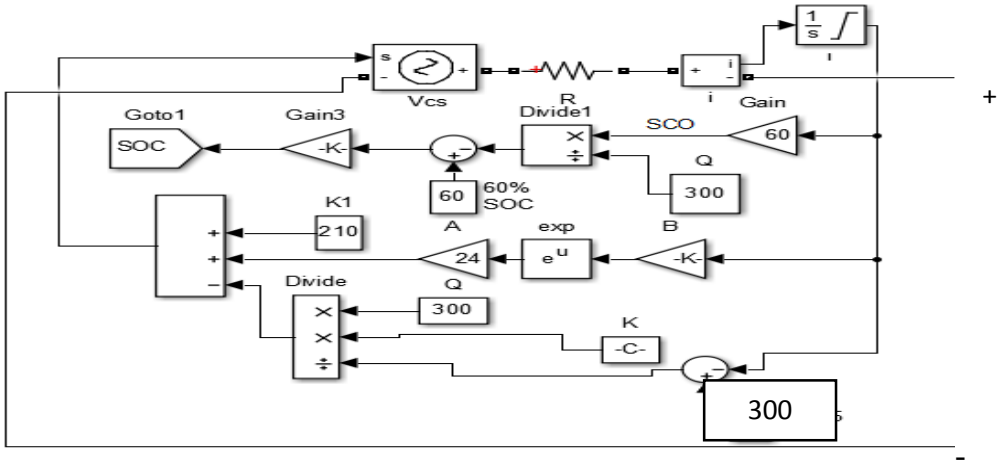

Fig.3.4. Battery

In section 2.3, the operation of boost-buck converter is stated and it is constructed from the SIMULINK model in Figure 3.5.

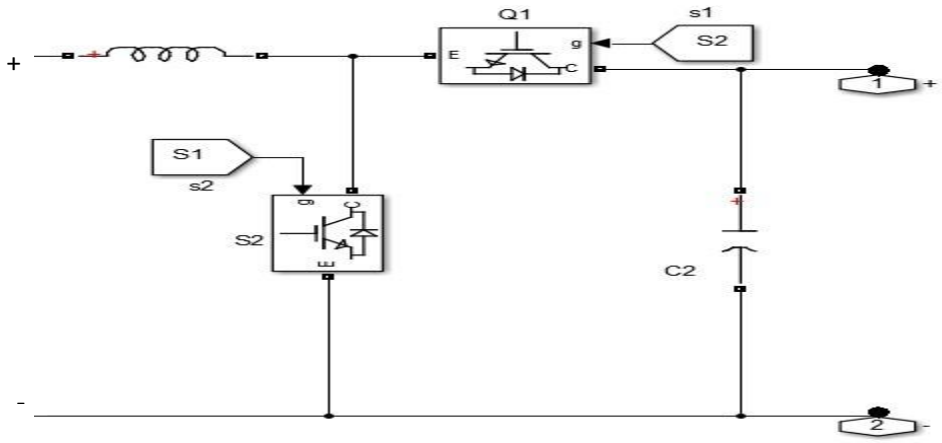

Fig.3.5. Boost-Buck Converter

The SIMULINK model of bi-directional inverter is shown in the following Figure. It's described in section 2.3.

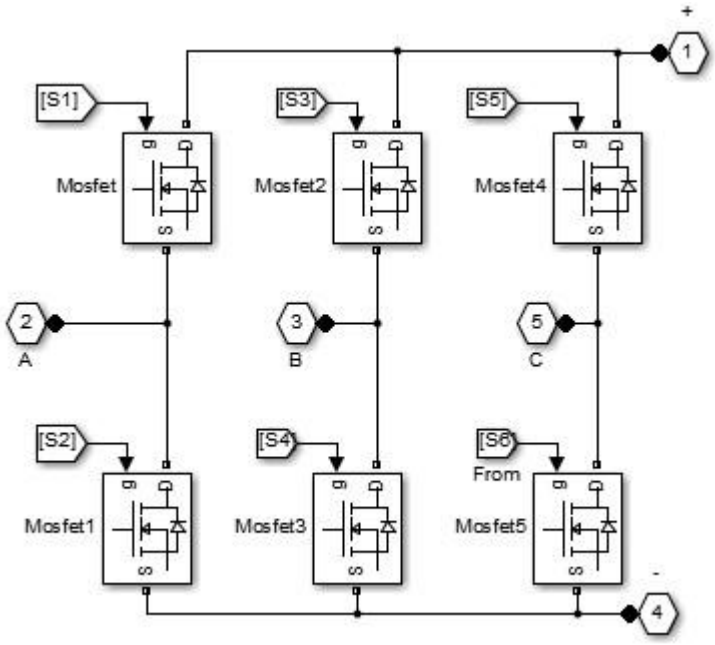

Fig.3.6 Bi-directional Inverter

The low pass filter is established in SIMULINK environment and it's detailed clarification in section 2.3.

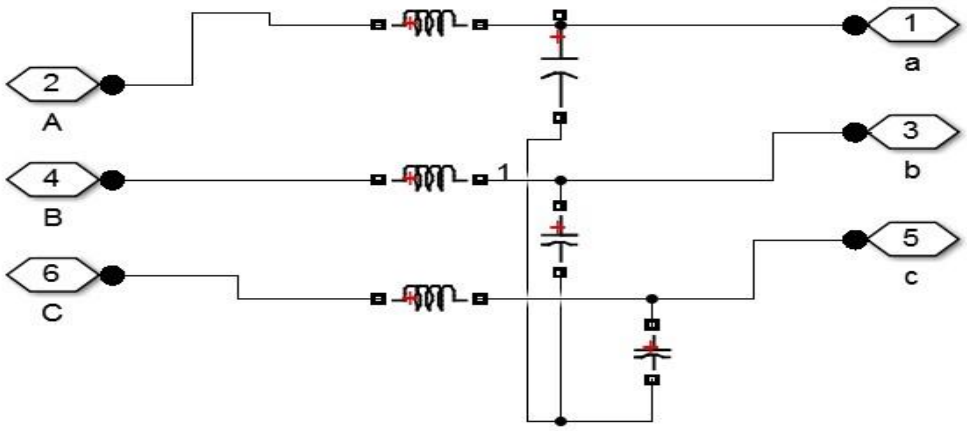

Fig 3.7. Low Pass Filter

Finally, the main V/f controller is built using library block, has the model show in Fig.3.8. In section 2.5, the operations of V/f controller have described.

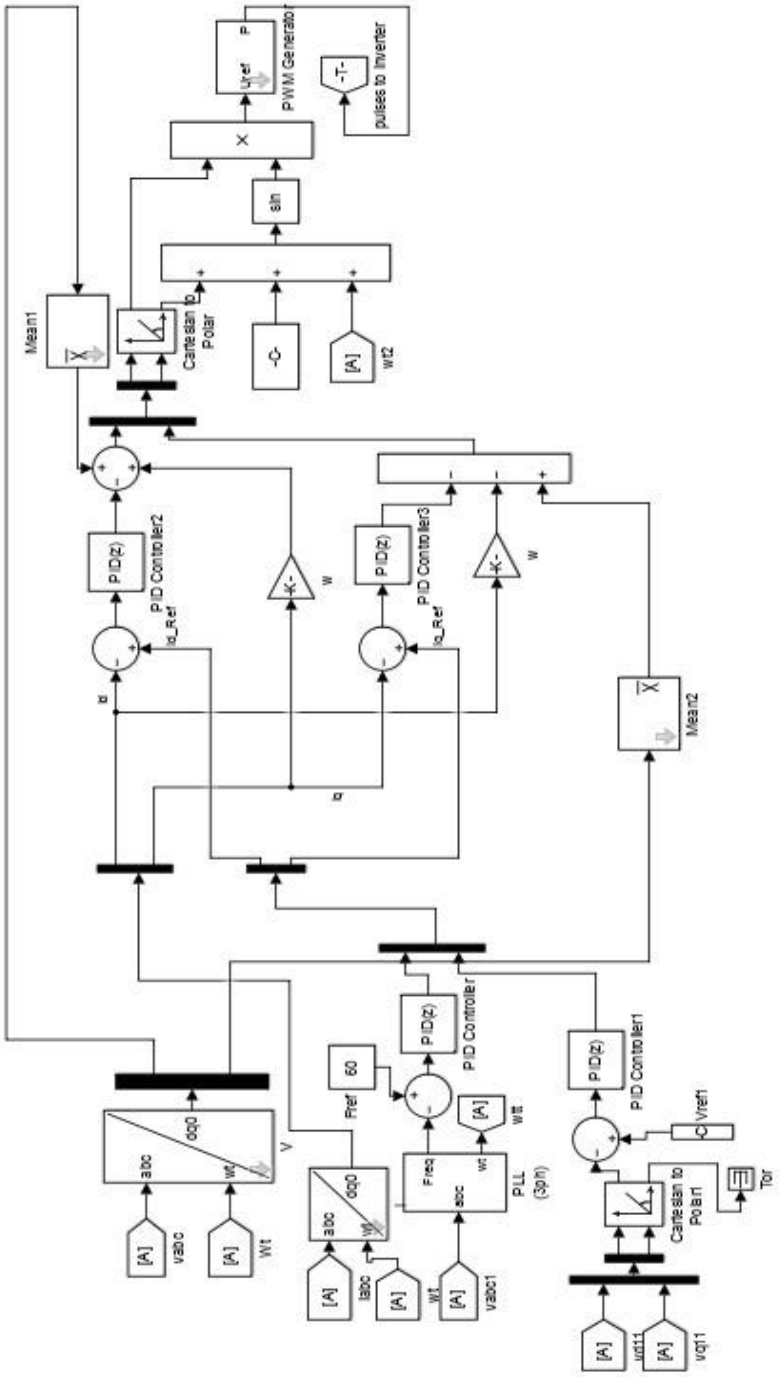

Fig.3.8. V/f Controller

The parameters in an IG for micro-turbine, which are used in Table 3.1, are shown in Fig 3.9.

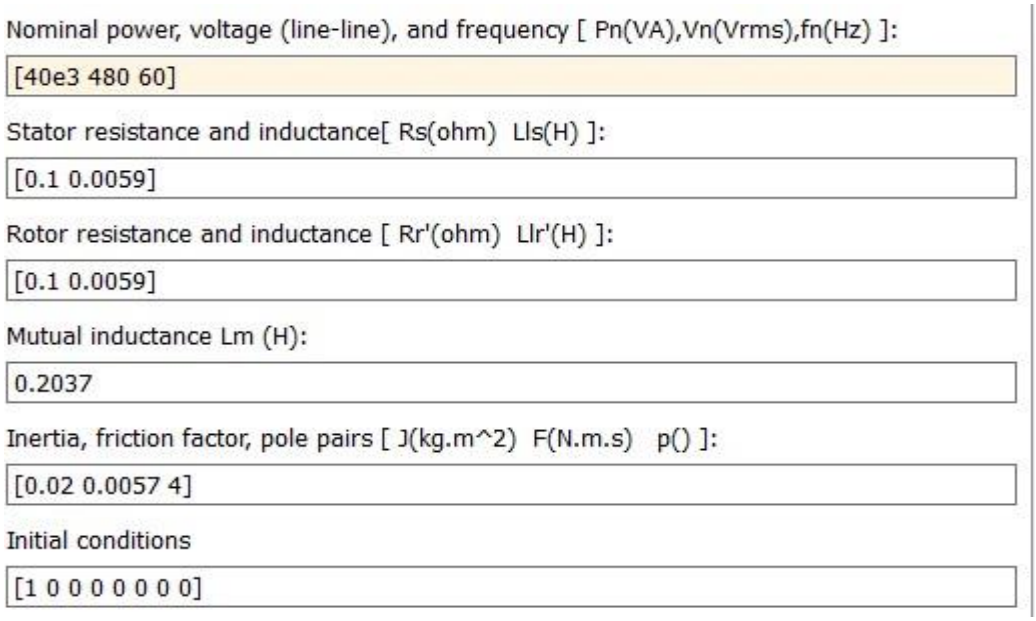

Fig.3.9. IG of micro-turbine

The IG of wind-turbine with its parameters, which correspond with Table 3.2 is presented in Fig.3.10.

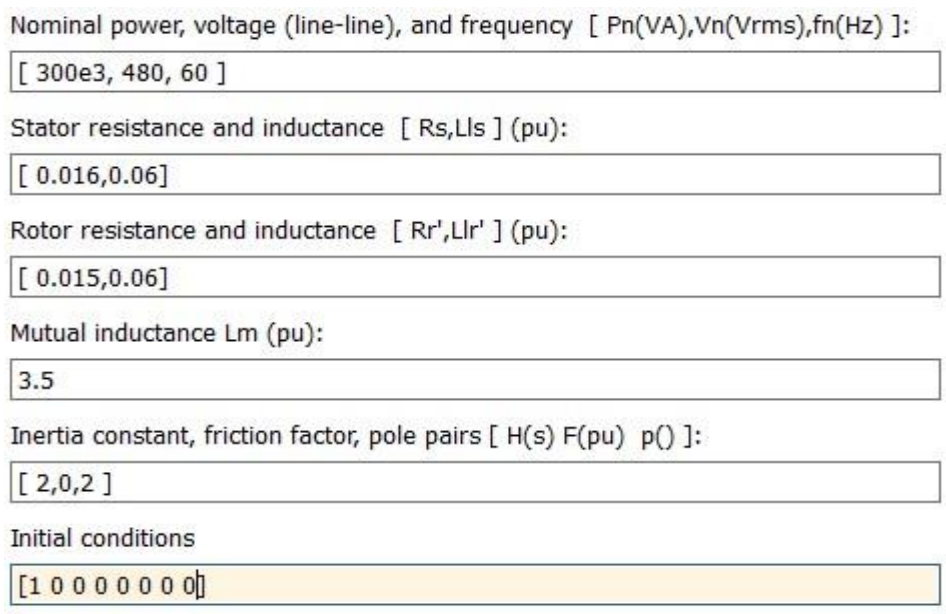

Fig.3.10 IG of wind-turbine

3.2 Simulation Parameters

Table 3.1. The parameters of induction generator for micro-turbine [16]

Parameters	Magnitude	Unit
P_{rated}	40	kW
P_{ref}	1 p.u	-
P_n	4	-
T_1	10	s
T_2	0.1	s
T_3	3	s
K_P	1	-
K_I	1.08	-
K_T	1	-
V_{rated}	480	v
V_{max}	1.2	-
V_{min}	0.1	-
L_{max}	1.2	-
L_m	0.2037	H
L_s	0.0059	H
L_r	0.0059	H
D_t	0.03	-
D_g	0.1	-
R_s	0.1	Ω
R_r	0.1	Ω

J	0.02	$kg.m^2$
F_g	0.0057	-

TABLE 3.2. The parameters of induction generator for wind turbine [14].

Parameters	Magnitude	Unit
P_{wt}	275	KVA
R_S	0.016	p.u
R_r	0.015	p.u
L_S	0.06	p.u
L_r	0.06	p.u
L_m	3.5	p.u
H	2	-
$F_{wt,sc}$	0	-
$P_{n,wt,sc}$	2	-
W_S	10	m/s
G_S	1800	rpm
F	60	Hz
P_m	275	kW
P_{sc}	300	KVA

TABLE 3.3. Battery Parameter

Parameters	Magnitude	Unit
B_{rated}	300	Ah
SOC	60%	-
$I_{discharge}$	30	A
R_b	0.016667	Ω
V_n	200V	V
Q_n	240	Ah
V_e	210	V
Q_e	60	Ah
V_f	234V	V
Q	300	Ah
Q_m	315	Ah

TABLE 3.4. Boost-Buck Parameter

Parameters	Magnitude	Unit
L	0.15e-3	H
C	62.4e-6	F
V_{dc}	400	V
F_S	2K	Hz

Table 3.5. Filter Parameter

Parameters	Magnitude	Unit
L_f	1.23e-3	H
C_F	8.9e-6	F
F_S	20000	Hz

Others parameters could be seen either in micro-turbine, synchronous condenser or a battery.

3.3 Simulation Results

Case 1. The wind-speed changed from 11 m/s to 9 m/s at constant load and the following results were obtained. The first configuration when battery and wind-turbine is considered, shows that the power from the wind-turbine decreases as a result of decrease in wind speed reduced. However, the battery compensates the power after 10s as shown in Fig.3.11.

In Fig 3.12, a voltage in a micro-grid reached the steady state after 13s.

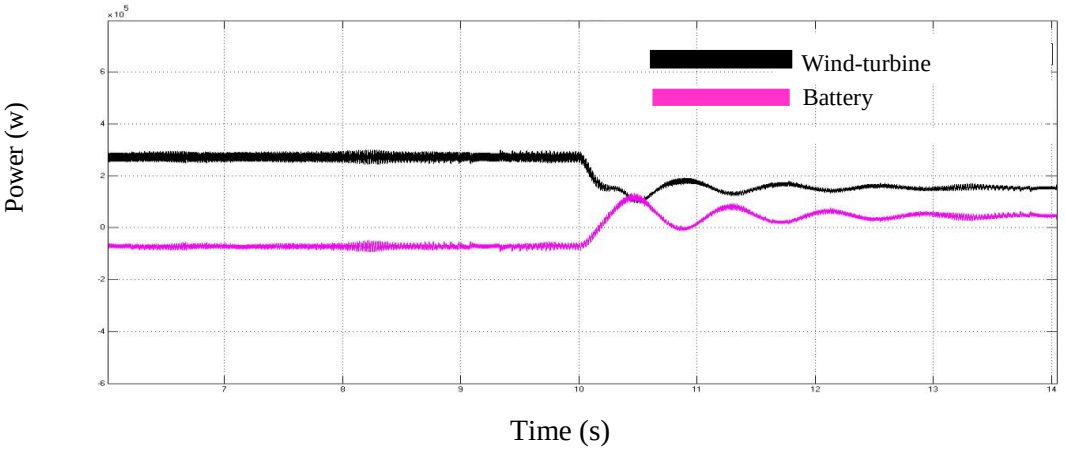

Fig.3.11. Power of μG for WT and Battery with wind speed change m

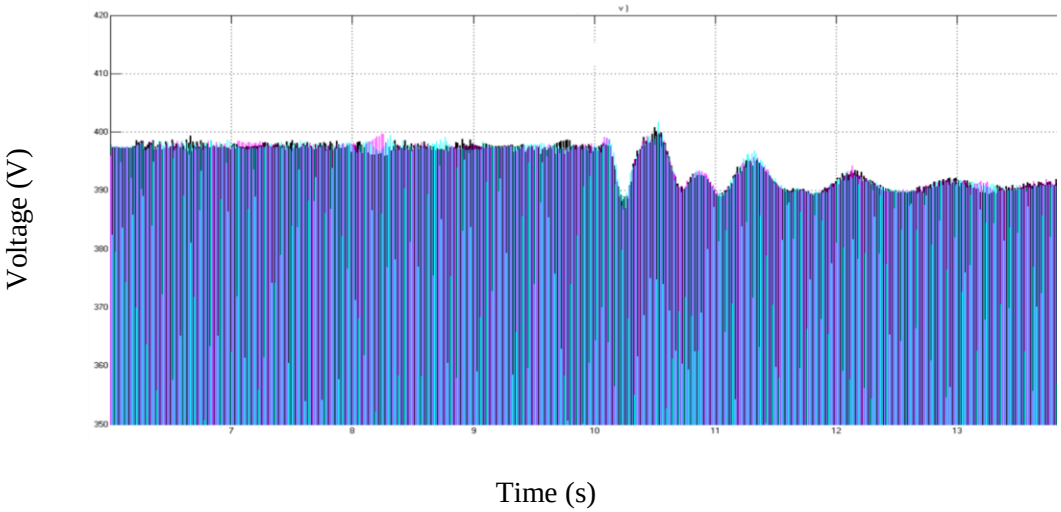

Fig.3.12. Voltage of μG for WT and Battery with wind speed change

Case 2: the wind-turbine, the micro-turbine and the battery worked together. At 10s, the wind-speed dropped and power generated from the wind-turbine decreased. In Fig.3.13, both power from micro-turbine and battery recovered the power lost from wind-turbine. Micro-grid voltage attained the steady state after 12s, shown in Fig.3.14.

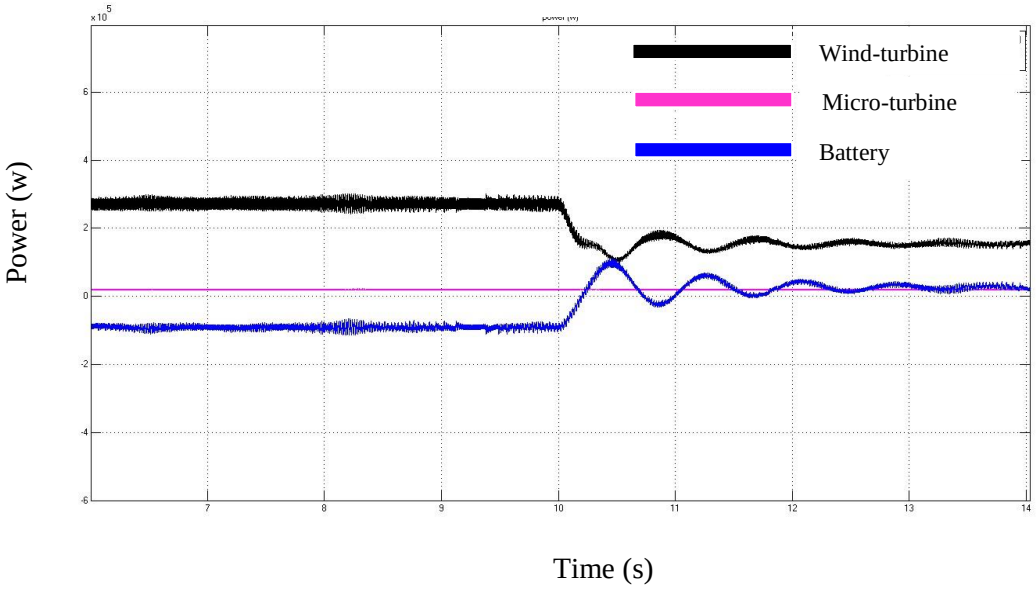

Fig.3.13. Power of µG for WT, MT and Battery with wind speed change.

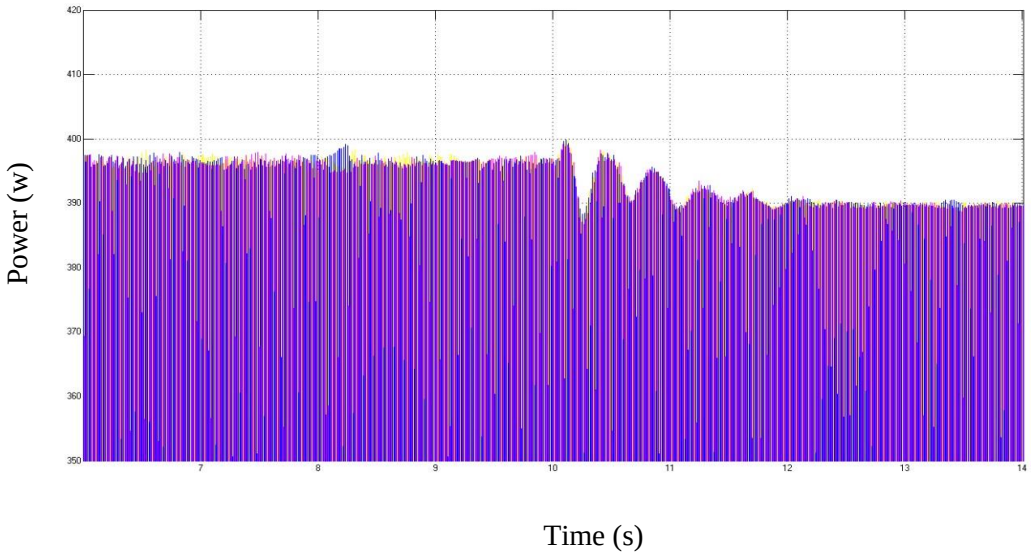

Fig.3.14. Voltage of µG for WT, MT and Battery with wind speed change

Case 3. At constant speed and change in loads from 250 to 350kW both power and voltage were observed. Initially, wind-turbine and battery arrangement was studied. In Fig.3.15, the battery compensated the increase in the power demand at 12s with steady state after 15s in micro-grid voltage, presented in Fig.3.16.

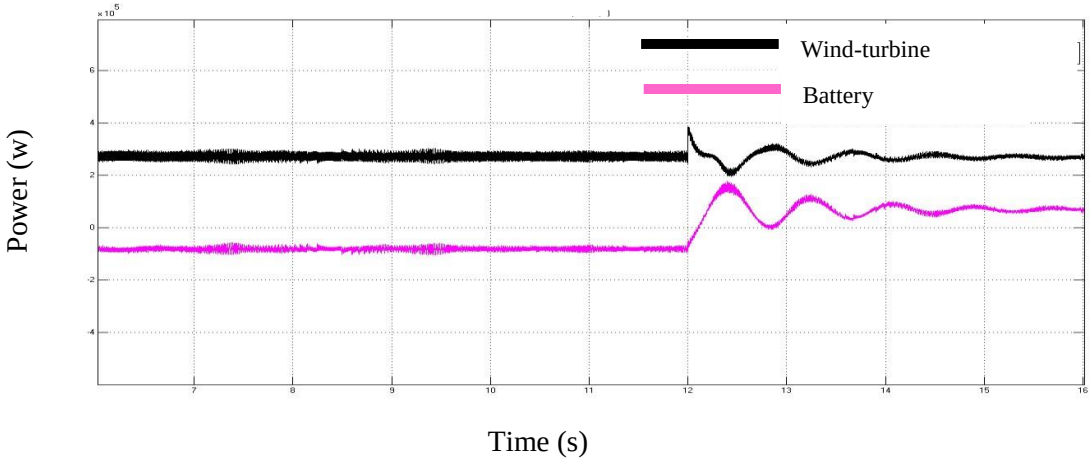

Fig.3.15. Power of μG for WT and Battery with load change

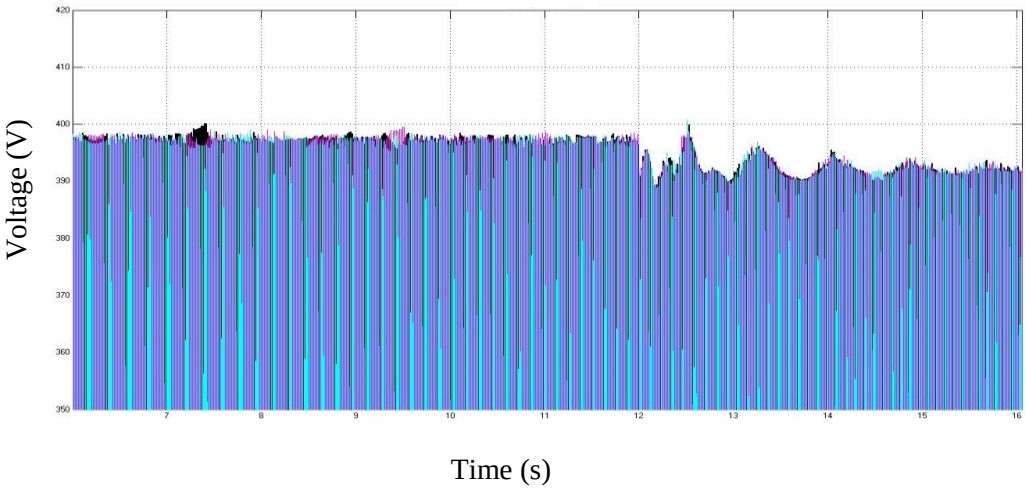

Fig.3.16. Voltage of μG for WT and Battery with load change

Case 4: all micro-sources and battery energy storage system were connected together. The load increased at 12s and both micro-turbine and battery balanced the power in the micro-grid, shown in Fig.3.17. In Fig.3.18, the voltage at micro-grid regained the steady state after 15.5s

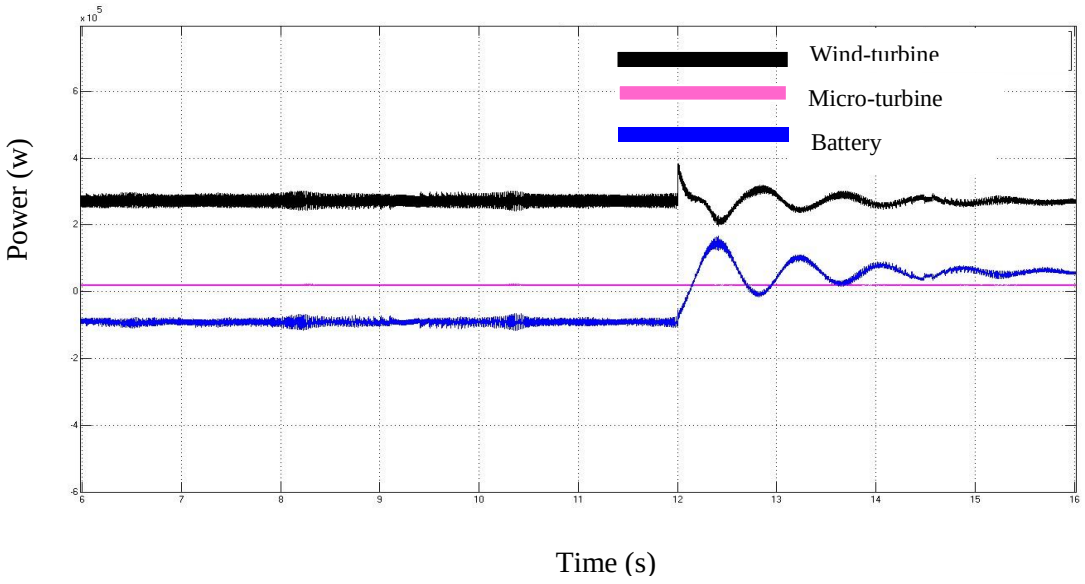

Fig.3.17. Power of μG for WT, MT and Battery with load change

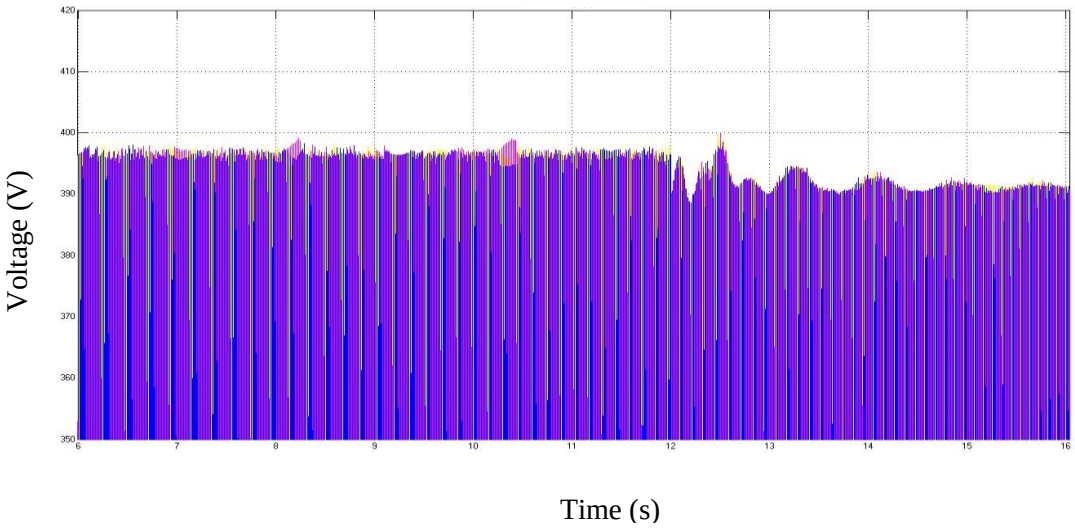

Fig.3.18. Voltage of μG for WT, MT and Battery with load change

4 CONCLUSION AND FUTURE WORK

The research was conducted successfully with remarkable outcomes. The simulation result of the μG model was obtained and the power control from different micro-sources in a μG autonomous running has been analyzed. The battery energy storage system got recharge when the micro-sources power is more than the load power and after few seconds' changes has occurred either from wind speed or load and more power is not available in the μG, battery discharged. The power control is capable of retaining any distraction in an autonomous μG and supplies a pure power to the load. For any μG to be manipulated in an acceptable way, one of μsources must to be communicated with an energy storage device. The power control and voltage control can be sustain at constant load. When the wind speed decreases from 11m/s to 9m/s, the power from wind turbine was shown to decrease but the power would be supplied from the battery to compensate for the lost. However, at constant speed of 11m/s, the load increase and thus increases in demand power of 140kW and thus the battery with a capacity of 100kW and 40kW of micro-turbine balanced for the lost.

Future Work

Though some form of control and optimization was achieved, there are still need to control the frequency in the μG. Another issues is with regard to the control of reference power for micro-turbine, which communicates with a battery through discharge and charge mode. In our model it is the only form of controls that were not achieved. Also failure in a micro-source should investigates. These are two potential direction for improvement upon this research work.

5 BIBLIOGRAPHY

[1] S. C. a. P. C. S. Chowdhury, Microgrid and Active Distribution Networks, United Kingdom: The Institution of Engineering and Technology, 2009, pp. 4-7.

[2] Xing Wu, Xiaogang Yin, Quan Wei, Yifan Jia, Jing Wang, "Research on Microgrid and its Application in China," *sientific research,* vol. 5, no. 171-176, p. 171/2, 2013.

[3] Nikos Hatziargyriou,Hiroshi Asano, Reza Iravani,and Chris Marnay, "Microgrid:An Overview of Ongoing Research, Development, and Demonstration Projects," IEEE power & energy magazine, 2007.

[4] Roman-Barri, M Cairo-Molins, I. Sumper, A.Sudria-Andreu, A, "Experience on the implementation of a microgrid project in Barcelona," in *IEEE*, Gothenburg, 11-13 october 2010.

[5] K. ISHIDA Y. SHIMOGAWA Y. SATO K. TAKANO T. IMAYOSHI , "Demonstration tests of microgrid systems using renewable energy for small remote islands," in *Kyushu Electric Power Co., Inc.*, Japan, 2012.

[6] "Wind/PV/Diesel Micro-Grid System Implemented in remote Islands in Republic of Maldives," in *ICSET*, Maldives, 2008.

[7] R. P. P. Lasseter, "Microgrid: A Conceptual Solution," in *PESC'04 Aachen*, Germany, 20-25 June 2004.

[8] S. M. I. a. X. Y. Zhenhua Jiang, "Active Power - Voltage Control Scheme for Islanding Operation of Inverter-Interfaced Microgrids," *National Science Foundation,* 2009.

[9] Rashad M. Kamel, Aymen Chaouachi, Ken Nagasaka, "Analysis of Transient Dynamic Response of Two Nearby," *scientific research,* vol. 1, pp. 39-53, 10 December ,2010.

[10] Rashad M. Kamel, Aymen Chaouachi, Ken Nagasaka , "Detailed Analysis of Micro-Grid Stability during Islanding," *scientific research,* vol. 3, no. 10.4236/eng.2011.35059, pp. 508-516, Received January 21, 2011; revised March 4, 2011; accepted April 6, 2011.

[11] Chamana, M. Bayne, S.B., "Modeling and control of directly connected and inverter interfaced sources in a microgrid," in *IEEE*, North American Power Symposium (NAPS), 2011, 4-6 Aug. 2011.

[12] Li, Bin Bao, Hailong ; Chen, Yao, "Simulation study on micro-grid coordinated control under islanding operation," in *Power Electronics and*

Motion Control Conference (IPEMC), 2012 7th International , Harbin, China, 2-5 June 2012.

[13] Gelu GURGUIATU1 Ionel VECHIU2 and Toader MUNTEANU1, "google," ESTIA-Recherche Bidart, [Online]. Available: http://www.icrepq.com/icrepq%2711/437-gurguiatu.pdf. [Accessed Friday April 2015].

[14] Syed Q. Ali1,Hany M. Hasanien2, "Frequency Control of Isolated Network with Wind and Diesel Generators by Using Adaptive Artificial Neural Network Controller," *International Review of Automatic Control*, vol. 5, no. 1974-6059, pp. 179-186, March 2012.

[15] Dr.Meenakshi mataray ,AP .Ms. Shamsha Keshwani, "Frequency Control of Isolated Network withWind and Diesel Generators by Using Frequency Regulator," *International Journal of P2P Network Trends and Technology (IJPTT)*, vol. 6, no. 2249-2615 , p. 34, 2014.

[16] R. K. a. B. Kermanshahi1, "Design and Implementation of Models for Analyzing the Dynamic Performance of Distributed Generators in the Micro Grid Part I: Micro Turbine and Solid Oxide Fuel Cell," in *Archive of SID*, tokyo, japan, June 2010.

[17] S. K. Nayak, "Performance Distributed Generation System in Utility Interconnected and Islanding Modes of Operation," *science*, vol. 02, pp. 60-63, 2013.

[18] Olivier Tremblay, Member IEEE, Louis-A. Dessaint, Senior Member IEEE, and Abdel-Illah Dekkich, "A Generic Battery Model for the Dynamic Simulation of Hybrid Electric Vehicles," 2007.

[19] B. Hauke, "Basic Calculation of a Boost Converter's Power Stage," Texas Instruments Incorporated, November 2009–Revised January 2014.

[20] A. P. a. Q. Pekik A. Dahono, "An LC Filter Design Method for Single-phase PWM Inverters," in *IEEE*, Ganesha No. 10, Bandung 40132, INDONESIA, Febuary, 1995.